Unusual Near-Horizon Cosmic-Ray-like Events Observed by ANITA-IV

P. W. Gorham,[1] A. Ludwig,[2] C. Deaconu,[2] P. Cao,[3] P. Allison,[4] O. Banerjee,[4] L. Batten,[5] D. Bhattacharya,[6] J. J. Beatty,[4] K. Belov,[7] W. R. Binns,[8] V. Bugaev,[8] C. H. Chen,[9] P. Chen,[9] Y. Chen,[9] J. M. Clem,[3] L. Cremonesi,[5] B. Dailey,[4] P. F. Dowkontt,[8] B. D. Fox,[1] J. W. H. Gordon,[4] C. Hast,[10] B. Hill,[1] S. Y. Hsu,[9] J. J. Huang,[9] K. Hughes,[4] R. Hupe,[4] M. H. Israel,[8] T. C. Liu,[11] L. Macchiarulo,[1] S. Matsuno,[1] K. McBride,[4] C. Miki,[1] J. Nam,[9] C. J. Naudet,[7] R. J. Nichol,[5] A. Novikov,[12,13] E. Oberla,[2] M. Olmedo,[1] R. Prechelt,[1] B. F. Rauch,[8] J. M. Roberts,[1] A. Romero-Wolf,[7] B. Rotter,[1] J. W. Russell,[1] D. Saltzberg,[14] D. Seckel,[3] H. Schoorlemmer,[15] J. Shiao,[9] S. Stafford,[4] J. Stockham,[12] M. Stockham,[12] B. Strutt,[14] M. S. Sutherland,[2] G. S. Varner,[1] A. G. Vieregg,[2] S. H. Wang,[9] and S. A. Wissel[16]

[1]*Department of Physics and Astronomy, University of Hawaii, Manoa, Hawaii 96822, USA*
[2]*Department of Physics, Enrico Fermi Institute, Kavli Institute for Cosmological Physics, University of Chicago, Chicago, Illinois 60637, USA*
[3]*Department of Physics, University of Delaware, Newark, Delaware 19716, USA*
[4]*Department of Physics, Center for Cosmology and AstroParticle Physics, The Ohio State University, Columbus, Ohio 43210, USA*
[5]*Department of Physics and Astronomy, University College London, WC1E 6BT London, United Kingdom*
[6]*Department of Mathematics, George Washington University, Washington, D.C. 20052, USA*
[7]*Jet Propulsion Laboratory, California Institute of Technology, Pasadena, California 91109, USA*
[8]*Department of Physics and McDonnell Center for the Space Sciences, Washington University in St. Louis, St. Louis, Missouri 63130, USA*
[9]*Department of Physics, Graduate Institute of Astrophysics, and Leung Center for Cosmology and Particle Astrophysics, National Taiwan University, Taipei 10617, Taiwan*
[10]*SLAC National Accelerator Laboratory, Menlo Park, California 94025, USA*
[11]*Department of Electrophysics, National Yang-Ming Chiao Tung University, Hsinchu 30010, Taiwan*
[12]*Department of Physics and Astronomy, University of Kansas, Lawrence, Kansas 66045, USA*
[13]*National Research Nuclear University, Moscow Engineering Physics Institute, Moscow 115409, Russia*
[14]*Department of Physics and Astronomy, University of California, Los Angeles, Los Angeles, California 90095, USA*
[15]*Max-Planck-Institute für Kernphysik, 69029 Heidelberg, Germany*
[16]*Department of Physics, Department of Astronomy and Astrophysics, Pennsylvania State University, University Park, Pennsylvania 16801, USA*

(Received 19 August 2020; revised 20 October 2020; accepted 12 November 2020; published 19 February 2021)

ANITA's fourth long-duration balloon flight in 2016 detected 29 cosmic-ray (CR)-like events on a background of $0.37^{+0.27}_{-0.17}$ anthropogenic events. CRs are mainly seen in reflection off the Antarctic ice sheets, creating a phase-inverted waveform polarity. However, four of the below-horizon CR-like events show anomalous noninverted polarity, a $p = 5.3 \times 10^{-4}$ chance if due to background. All anomalous events are from locations near the horizon; ANITA-IV observed no steeply upcoming anomalous events similar to the two such events seen in prior flights.

DOI: 10.1103/PhysRevLett.126.071103

Antarctic ice has been recognized for decades as an ideal natural dielectric target for the detection of cosmic neutrinos via the Askaryan effect, which leads to coherent radio Cherenkov impulses from particle cascades in dielectric materials [1–3]. The Antarctic Impulsive Transient Antenna (ANITA) instrument was designed to exploit this effect by broadband monitoring of several million km^3 of ice in the 200–1200 MHz band from the stratosphere during a long-duration balloon flight [4].

During prior flights, ANITA also found that several dozen ultrahigh-energy (UHE) cosmic-ray (CR) events were also detectable from the payload's stratospheric vantage point [5]. Cosmic-ray extensive air showers (EAS) in the geomagnetic field produce 1°-beamed radio impulses via a charge acceleration mechanism tied to the magnetic Lorentz force $\mathbf{F}_{\mathcal{L}} = q\mathbf{v} \times \mathbf{B}_{\text{geo}}$ for particle charge q, velocity $\mathbf{v}$, and geomagnetic field $\mathbf{B}_{\text{geo}}$. In CR EAS, this mechanism dominates over the Askaryan effect, leading to signals with strong correlations in polarization to the local geomagnetic field where the shower propagated.

For the fourth flight of ANITA, we pursued two separate analysis paths, one for neutrinos interacting below the ice surface and detected via the Askaryan channel and one for CR or CR-like events detected via the EAS channel. Results of the ANITA-IV analysis for neutrino events via the Askaryan channel are reported elsewhere [6].

ANITA's effective area for CR detection is not competitive with other large ground-based CR observatories [7], but its

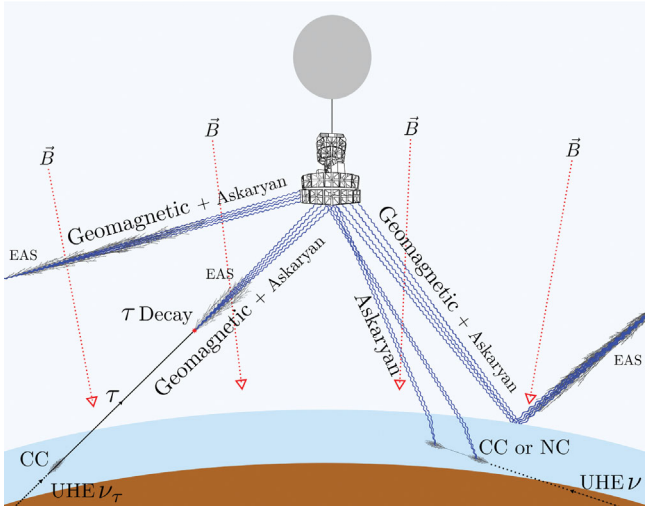

FIG. 1. Diagram of ANITA-IV signal channels, in the near-vertical Antarctic geomagnetic field. Geomagnetic signals appear from CRs either directly or in reflection and include a small Askaryan radiation component. Askaryan signals dominate the under-ice neutrino channel and can arise from multiple showers due to both primary and secondary interactions. Geomagnetic signals can also arise from EAS initiated by τ-lepton decay after ν_τ charged-current (CC) interactions within the ice.

field of view from the stratosphere does provide access to geometries that ground-based CR observatories cannot see. CRs that arrive tangential to Earth's surface may interact in the stratosphere, and the EAS may be confined completely to the stratosphere, never intersecting with Earth's surface. Such stratospheric events appear to ANITA as a CR radio source near, but just above the horizon, in a thin band of atmosphere observed at the limb of Earth. In contrast, the large majority of CRs which arrive on trajectories that do intersect Earth appear to ANITA in reflection off the relatively radio-smooth surface of the ice. The reflection causes a phase inversion in the CR waveform, providing a clear distinction between these downgoing CRs and their stratospheric counterparts. Figure 1 provides a schematic overview of the various possible signal channels for ANITA.

In each of two prior ANITA flights where CR observations were made, single anomalous CR events were observed at payload arrival angles of $-27°$ [8] and $-35°$ [9] relative to horizontal. The polarity of these events was not phase inverted as was the case for all of the other (several dozen) reflected CRs observed in the below-horizon angular region. These CR-like events had low probability of being background, especially for the unusual event observed by ANITA-III [9]. No natural origin for the noninverted polarity has yet been confirmed, though several have been suggested [10,11] and, in some cases, largely excluded by ANITA [12]. IceCube has also published constraints on potential astrophysics sources for these events [13].

ANITA-IV was launched on December 2, 2016, reaching a float altitude of about 40 km several hours later, and flew in the Antarctic polar vortex for 28 days until the flight was terminated on December 29, 2016, about 160 km from the South Pole. The data recording live time averaged ~90% during the flight, yielding 24.5 days net.

The blind analysis [14] used to extract the ANITA-IV CR sample followed closely the methods detailed for ANITA-III [9] and those described for the neutrino analysis [6]. The CR analysis methods included using cross-correlation with a CR waveform template and polarization correlation with the local geomagnetic field.

Events from large active bases—McMurdo, West Antarctic Ice Sheet, South Pole, etc.—are excluded as signal. A statistical sideband sample, extracted from excluded events with known anthropogenic associations, was used to estimate the anthropogenic background, which is assumed to "leak" out from weak sources into isolated single events. The final signal analysis is still blind to polarity at this stage, and a detailed analysis of the anthropogenic sample gives a background estimate of $0.37^{+0.27}_{-0.17}$ events, for events of both polarities in the final CR sample. By comparison, the thermal radio noise background contribution is negligible, $\sim 5 \times 10^{-7}$ events.

The complete unblinded sample of isolated events showed 29 candidates distributed widely across the continent, as shown in Fig. 2 (top) [15,16]. They are consistent with CRs in their template correlation coefficient and geomagnetic parameters (Fig. 2, bottom). The events were observed at arrival angles of $-36°$ to $-5.5°$ with respect to horizontal (the horizon appears at about $-6°$ relative to horizontal from stratospheric altitudes). The two events observed from above the horizon are identified as candidate stratospheric EAS, a class of extensive air showers first observed by ANITA [5].

Prior to determining polarity, the events are processed to form coherently summed waveforms (CSWs), created by combining signal from 15 antennas that contain the source within their field of regard with group delays that match the source direction. This process is known as *beam forming* in radio interferometric usage. ANITA's beam forming typically improves the signal-to-noise ratio (SNR) by a factor of 3 compared to the original detection.

ANITA's CSWs show a time-dispersed shape caused by the variable group delay of different frequency components passing through the ANITA antenna, receiver, and digitizer systems. Each intrinsic CR impulse is, therefore, convolved with this system impulse response, inducing both phase and amplitude distortion in the received signal. This impulse response also varies during the flight, due to changes in the frequency-notch configuration as we work to suppress electromagnetic interference [17].

Calibration errors in portions of the global analysis discovered after the initial CR unblinding required that the data be reanalyzed [17]. The final subsequent polarity analysis was done after reblinding of the data, including blinding of event number, randomizing event order, and

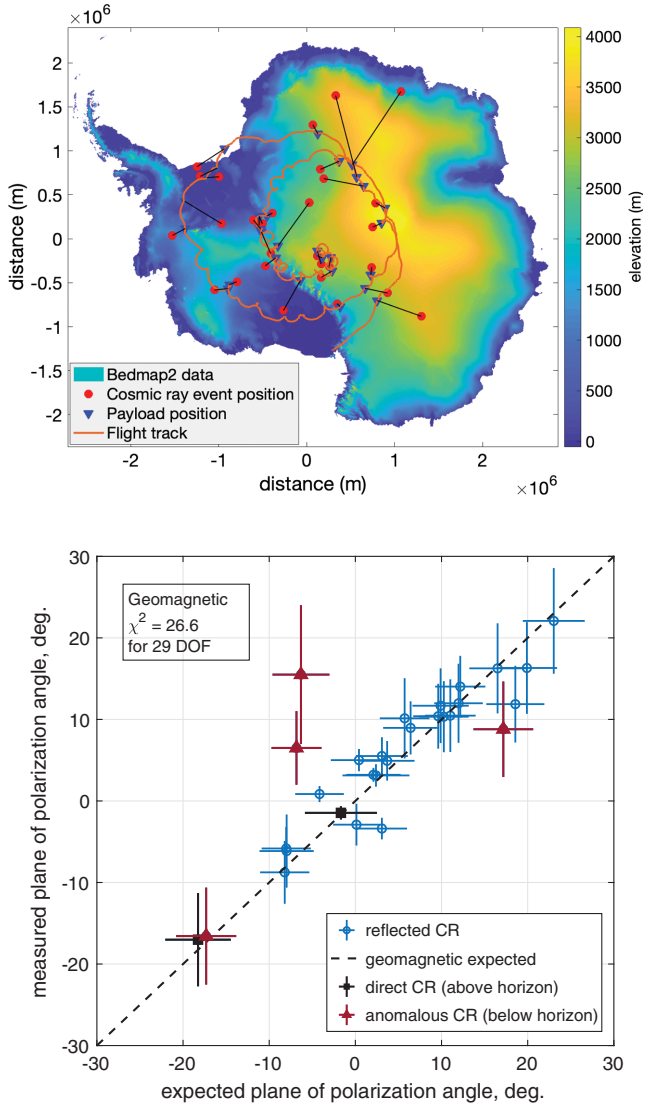

FIG. 2. Top: ANITA-IV flight path and location of payload and apparent event source location and ice surface elevation above sea level for each of the 29 events in the final CR sample. Bottom: Geomagnetic correlation of 29 candidate events revealed in our CR analysis.

applying a random polarity factor to all CR events as the polarity metrics were determined.

Polarity is unrelated to the polarization state of the event. Polarity refers to the instantaneous phase of the electric field, whereas polarization refers to the plane of the field oscillation. After deconvolution of the system response [17], CR events observed by ANITA vary from nearly unipolar, to dominant bipolar, and some subdominant tripolar events.

Polarity of a unipolar pulse is determined by the sign of the pole. In bipolar events, the polarity is indicated by the order of the two primary poles; for ANITA data, we find that the sign of leading main pole in a bipolar event determines the polarity. Tripolar components for ANITA events are always subdominant to unipolar or bipolar shapes and do not affect the polarity determination in general.

After unblinding polarity, we find two events with indeterminate polarity; coincidentally, both had payload arrival angles of −14.8°. After further investigation, one of these events, 74197411, was found to be adversely affected by high-frequency interference of likely anthropogenic origin. Filtering this interference revealed that the polarity was that of a normal CR. For the other event, 88992443, the polarity could not be resolved and remains indeterminate. This event has a waveform quite different from all other CRs and has the lowest SNR of any CR observed. Both of these events are excluded from these analyses; their data are provided elsewhere [17].

For the remaining 27 events,the confidence level (C.L.) for polarity determination was found by Monte Carlo methods to be ∼99% for one event (19848917) and ≥ 99.99% for the remainder. For 19848917, the ∼1% chance of polarity misidentification appears to be due to limitations of our algorithm rather than intrinsic uncertainty in this event's polarity.

Of the remaining 27 events, 23 events have the normal CR polarity expected from their geometry. Figure 3 shows

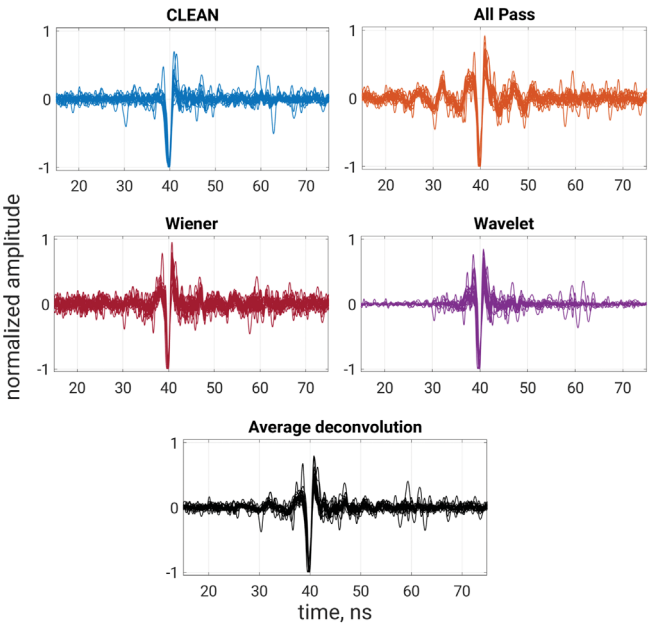

FIG. 3. Normalized overlays of the 21 normal reflected CR in our sample, in each of the four deconvolution methods used, as noted by the title for each pane. CLEAN [23] is a time-domain method based on iterative correlation and subtraction of the impulse response [24,25]. The all-pass method applies simple Fourier-division deconvolution to the phases only. Wiener deconvolution uses a noise-optimized Fourier deconvolution method for both phases and amplitudes [26]. The wavelet method [27,28] uses wavelet, rather than Fourier, basis functions for the deconvolution. The bottom plot gives the normalized average waveform of the four methods.

TABLE I. Preliminary list of stratospheric CR and possible anomalous CR-like events seen by ANITA-IV.

	mm dd hh mm ss	Apparent source location	Elev. angle[a]	Horizon angle[a]	Azimuth	Payload location	Type[c]	Energy[d]
Event #	UTC 2016	Lat.°, lon.°, alt., m	degrees	degrees	degrees	Lat.°, lon.°, alt., km		EeV
4098827	12 03 10 03 27	−75.71, 123.99, 3184	-6.17 ± 0.21	-5.92 ± 0.020	337.70	−80.157, 131.210, 38.86	NI	1.5 ± 0.7
9734523	12 05 12 55 40	−71.862, 32.61, 19 000[b]	-5.64 ± 0.20	-5.95 ± 0.020	2.01	−80.9, 31.6, 39.25	AH	···
19848917	12 08 11 44 54	−80.818, −79.87, 758	-6.71 ± 0.20	-6.06 ± 0.020	194.34	−76.66, −72.86, 38.97	NI	0.9 ± 0.5
50549772	12 16 15 03 19	−83.483, 14.73, 2572	-6.73 ± 0.20	-5.92 ± 0.020	234.08	−81.95, 47.29, 38.52	NI	0.8 ± 0.3
51293223	12 16 19 08 08	−74.800, 11.43, 18 600[b]	-5.38 ± 0.24	-5.85 ± 0.020	306.45	−81.7, 39.2, 37.53	AH	···
72164985	12 22 06 28 14	−86.598, 0.35, 2589	-6.12 ± 0.10	-5.93 ± 0.020	140.03	−86.93, −104.29, 38.58	NI	3.9 ± 2.5

[a]Both the observed elevation angle and the apparent horizon here include radio refraction, which lifts the apparent horizon about 0.1°.
[b]The source elevation (in the stratosphere) and the given source position are estimates of the approximate location of EAS maximum for these direct stratospheric CR events, determined by using the average column depth to shower max for EeV CRs.
[c]AH: above horizon, direct CR. NI: Noninverted CR-like event, below horizon.
[d]Energy computable for below-horizon events only; above-horizon simulations are beyond our scope in this report. Errors include both statistical and systematic effects.

an overlay of the 21 events with polarity consistent with reflection from the ice sheet surface, the most common type of CR observed by ANITA. Each of the panes shows the results of the different deconvolution methods [17] along with an overlay of the average of all four waveform methods. This final waveform average, chosen for robustness to systematics in the individual deconvolutions, was used to determine the polarity in all events.

In addition to the 23 normal reflected CR, four events near the horizon had noninverted polarity, inconsistent with a reflected CR, though their source directions were on the ice sheets. Table I shows parameters for the four near-horizon and two above-horizon events. Pointing parameters in these cases used weighted averages of the pointing determined from interferometric maps of both polarizations where there was sufficient SNR. Under the assumption these are CR showers, the table includes estimates of the energy based on scaling from our prior CR energy measurements [7].

The stratospheric events 9734523 and 51293223 are consistent with CRs developing at altitudes of 18–19 km above Earth's surface. As such, they enter Earth's atmosphere at distances beyond the physical horizon, and the resulting particle cascades develop over hundreds of kilometers through the rarefied stratosphere at such altitudes. Estimation of their energies will have to await detailed simulations of these rather extreme form of EAS. These two above-horizon events appear at angles of 0.3° and 0.47° above the horizon, respectively. In ANITA-III, we observed one other stratospheric event at ∼0.4° above the horizon and several at larger angles, but none closer than this.

For the events summarized in Table I, Fig. 4 shows the CLEAN deconvolutions scaled to give their incident electric field strength at the ANITA payload. Here the subdominant Vpol waveform component was added coherently to the Hpol component to produce the best estimate of the intrinsic field strength of the incident pulse in the plane of polarization. Systematic errors on the field strength are estimated to be ∼30%. The plot background colors indicate events from above horizon (pale blue) or below horizon (white). The central segments of the waveforms annotated in solid orange show the primary pole (for unipolar) or poles (for bipolar) that determine the polarity; dot-dashed lines show the off-peak waveforms and thermal noise. In laboratory tests using known signals plus thermal noise, CLEAN gave the most consistent recovery of the intrinsic waveform in the presence of noise, and thus we use the CLEAN waveform for the estimates in Fig. 4.

Event 4098827 had significant loss of bandwidth due to the three notch filters used to suppress anthropogenic interference for this event, and, although the deconvolution

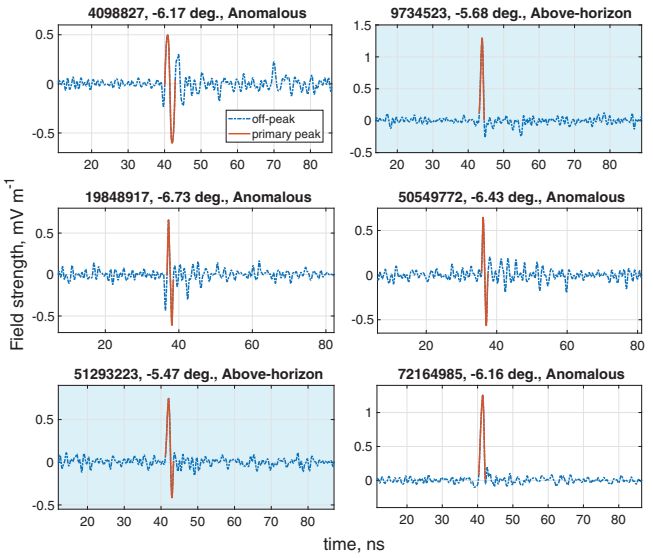

FIG. 4. The incident field strength vs time for the six near-horizon events, all of which have the same (noninverted) polarity: two above-horizon (pale blue background) and four below-horizon (white background) with anomalous polarity. These plots use the CLEAN deconvolution method as the waveform estimate.

recovers a portion of this signal via interpolation, the narrower effective bandwidth of this event is reflected in the larger number of zero crossings in the resulting waveform. Despite this, 4098827's polarity is in this case known with confidence, due to fortuitous observation of a normal three-notch-filter CR event [17] with a very similar waveform and which had inverted polarity with respect to this event.

In addition to the dedicated CR analysis, a separate neutrino-focused analysis chain based only on the impulsive nature of events and spatial isolation of their locations also found the majority of the CRs, independently confirming the efficacy of the CR methods [29]; further details are given in Supplemental Material [17].

In Table I, events 4098827 and 72164985 just below the horizon, by about 0.2°, about one and two standard deviations, respectively, for these two events. The standard error in angle given depends on their SNR, determined from ground-to-payload calibration pulsers during the flight. Both of these events thus have a non-negligible statistical chance to be due to stratospheric CRs misidentified as below-horizon events. To assess the chance of such a misidentification, we must consider the effects of grazing incidence rf propagation in the near-horizon atmosphere.

A detailed analysis of the effects of near-horizon propagation, including the use of GPS occultation data [30,31], indicates that the refractivity gradient can lead to significant phase distortion if the ray paths fall within 1 km of the surface, a region that is comparable to the size of the first Fresnel zone for ANITA's geometry [17]. Although we do not have direct measurements of the tropospheric parameters in the region that these events were observed, measurements taken at the South Pole indicate that spatial variations in the index of refraction observed in this near-surface atmosphere would lead to variations in the path delay across the wave fronts and loss of coherence at higher frequencies.

Such a loss of coherence does not appear consistent with our observations [17]. This suggests that, if 4098827 and 72164985 arise from misidentified above-horizon CRs, they require a true source direction that is $\gtrsim 0.1°$ above the horizon to preserve the observed coherence of the events. This requirement reduces the likelihood of an origin due to pointing fluctuations.

In addition to these propagation considerations, we have also considered the effects of a residual unknown $\pm 0.1°$ systematic pointing bias that might offset the apparent location of the events relative to their true direction. Evidence from our calibration and other data does not exclude possible bias at this level.

We exclude one effect which can produce grazing-incidence, below-horizon images of an above-horizon source: the so-called *inferior mirage* effect. This well-known manifestation is due to a near-surface refractive inversion layer. Under typical conditions, it produces inverted reflections, inconsistent with our observations. There are, however, reports of noninverted inferior mirages; careful study of the optics of these [32] shows that such images are the result of coherent surface concavities on a scale very long compared to the wavelength. In effect, the surface curvature mimics a concave ellipsoidal mirror, with one of its foci between the source and observer, thus causing an additional image inversion that cancels the reflection inversion. We have carefully searched ice-surface altimetry data [16] for evidence of such features for each of the four events, and none show surface altimetry consistent with this.

To estimate the overall significance of observing these four events given the anthropogenic background estimate, the chance for statistical polarity misidentification, and the chance for misreconstruction of the event direction, we performed two independent statistical simulations, each of which vary parameters for all 27 CRs with determined polarities, tabulating how often the outcomes randomly produce four or more such events in any combination. We allow variations for all types of systematic error noted above: a pointing bias, a propagation restriction, and polarity misidentification, to provide conservative bounds on the significance.

Both simulations gave consistent results, indicating a p-value range of

$$(3.7 \times 10^{-3}) \geq p \geq (7.5 \times 10^{-5})$$

equivalent to $(3.3 \pm 0.5)\sigma$ significance in Gaussian statistics [17]. While this C.L. is not adequate to conclude that these events may not be some combination of the different backgrounds, it is suggestive of a new class of CR-like events with Earth-skimming geometry.

ANITA-IV's sensitivity exceeded that of any prior ANITA flight. Three of these four events are near the threshold of sensitivity and would not have been observed previously. Currently, there is no radio EAS simulation that can treat events propagating in these very extreme conditions where a full-wave physical-optics solution is necessary. Such full-wave simulations with scales that can match the ANITA geometry are currently beyond the computing capabilities available for this work and will require a follow-up investigation to understand ANITA's acceptance to near-horizon EAS and any relevant near-horizon propagation effects that may impact the significance of the observation.

If such events arise from unexpected, but potentially mundane physical optics in the cryosphere or from other atmospheric or ice-topographic effects, it is crucial for these effects, which constitute a potential background for future experiments, to be explored in detail. Orbital and suborbital missions such as POEMMA [33] and PUEO [34], and ground-based experiments such as GRAND [35], which will specifically explore the potential τ-lepton neutrino

channel with much higher sensitivity, stand to benefit from a better understanding of all aspects of this process.

While the significance of the data does not yet require it, we anticipate the question of a possible particle physics origin for these events. The four near-horizon events are not inconsistent with EAS initiated by τ-lepton decay after emergence of the τ from a charged-current neutrino event in the ice along the track direction. Because their track directions are near tangential, the parent ν_τ would not suffer significant attenuation in Earth, a problem that appeared to exclude a standard-model neutrino origin for the steeply arriving anomalous events observed in earlier ANITA flights [36].

Thus, it is possible that one or more of these events can arise from an EAS generated by τ-lepton decay. However, to avoid saturating diffuse flux bounds, a transient point-source neutrino fluence is more likely than a steady-state diffuse flux, as is commonly assumed for UHE cosmogenic neutrinos. ANITA's point-source effective area for τ-lepton-generated EAS is maximal at the horizon, of the order of 0.1 km^2 at EeV energies, including the neutrino cross section and τ survival and decay effects. The implied UHE integral ν_τ fluence in this case, assuming an astrophysical transient event with a timescale of 1000 s or less, is of the order of 10 per km^2 above 3 EeV, which appears allowed by all current bounds on transients at these energies. Further work on understanding potential sensitivity to such events by other experiments is forthcoming.

ANITA-IV was supported by NASA Grant No. NNX15AC24G and related grants. We thank the staff of the Columbia Scientific Balloon Facility for their generous support. This work was supported by the Kavli Institute for Cosmological Physics at the University of Chicago. Computing resources were provided by the Research Computing Center at the University of Chicago and the Ohio Supercomputing Center at The Ohio State University. O. B. and L. C.'s work was supported by collaborative visits funded by the Cosmology and Astroparticle Student and Postdoc Exchange Network (CASPEN). S. A. W. thanks the Cal Poly Frost Fund and the CSU Research, Scholarship, and Creative Activity (RSCA) Grant Program. The University College London group was also supported by the Leverhulme Trust. The National Taiwan University group is supported by Taiwan's Ministry of Science and Technology (MOST) under its Vanguard Program No. 106-2119-M-002-011.

[1] G. A. Askaryan, Excess negative charge of an electron-photon shower and its coherent radio emission, JETP **14**, 441 (1962); **21**, 658 (1965).

[2] D. Saltzberg, P. Gorham, D. Walz, C. Field, R. Iverson, A. Odian, G. Resch, P. Schoessow, and D. Williams *et al.*, Observation of the Askaryan Effect: Coherent Microwave Cherenkov Emission from Charge Asymmetry in High-Energy Particle Cascades, Phys. Rev. Lett. **86**, 2802 (2001).

[3] P. W. Gorham, S. W. Barwick, J. J. Beatty, D. Z. Besson, W. R. Binns, C. Chen *et al.* (ANITA Collaboration), Observations of the Askaryan Effect in Ice, Phys. Rev. Lett. **99**, 171101 (2007).

[4] P. W. Gorham *et al.* (ANITA Collaboration), The Antarctic impulsive transient antenna ultra-high energy neutrino detector: Design, performance, and sensitivity for the 2006-2007 balloon flight. Astropart. Phys. **32**, 10 (2009).

[5] S. Hoover, J. Nam, P. W. Gorham, E. Grashorn, P. Allison, S. W. Barwick *et al.* (ANITA Collaboration), Observation of Ultra-high-energy Cosmic Rays with the ANITA Balloon-borne Radio Interferometer, Phys. Rev. Lett. **105**, 151101 (2010).

[6] P. W. Gorham *et al.* (ANITA Collaboration), Constraints on the ultra-high energy cosmic neutrino flux from the fourth flight of ANITA, Phys. Rev. D **99**, 122001 (2019).

[7] H. Schoorlemmer *et al.* (ANITA Collaboration), Energy and flux measurements of ultra-high energy CRs observed during the first ANITA flight, Astropart. Phys. **77**, 32 (2016).

[8] P. W. Gorham *et al.* (ANITA Collaboration), Characteristics of Four Upward-pointing Cosmic-ray-like Events Observed with ANITA, Phys. Rev. Lett. **117**, 071101 (2016).

[9] P. Gorham *et al.* (ANITA Collaboration), Observation of an Unusual Upward-going Cosmic-ray-like Event in the Third Flight of ANITA, Phys. Rev. Lett. **121**, 161102 (2018).

[10] K. D. de Vries and S. Prohira, Coherent Transition Radiation from the Geomagnetically Induced Current in Cosmic-Ray Air Showers: Implications for the Anomalous Events Observed by ANITA, Phys. Rev. Lett. **123**, 091102 (2019).

[11] I. Shoemaker, A. Kusenko, P. Kuipers Munneke, A. Romero-Wolf, D. Schroeder, and M. Siegert, Reflections on the anomalous ANITA events: The Antarctic subsurface as a possible explanation, Annals of Glaciology **61**, 92 (2020).

[12] D. Smith *et al.* (ANITA Collaboration), Experimental tests of sub-surface reflectors as an explanation for the ANITA anomalous events, arXiv:2009.13010.

[13] M. G. Aartsen *et al.* (IceCube collaboration), A search for IceCube events in the direction of ANITA neutrino candidates, Astrophys. J. **892**, 53 (2020).

[14] A. Ludwig, Radio detection of ultra-high energy neutrinos, Ph.D. thesis dissertation, University of Chicago, 2019, https://knowledge.uchicago.edu/record/1842?ln=en.

[15] C. A. Greene *et al.*, Antarctic mapping tools for Matlab, in *Computers & Geosciences* (Elsevier BV, New York, 2017), vol. 104, pp. 151–157, https://doi.org/10.1016/j.cageo.2016.08.003.

[16] P. Fretwell *et al.*, Bedmap2: Improved ice bed, surface and thickness datasets for Antarctica, The Cryosphere **7**, 375 (2013).

[17] See Supplemental material at http://link.aps.org/supplemental/10.1103/PhysRevLett.126.071103 describing the more specialized details of these analysis, which includes Refs. [18–22].

[18] R. Smída *et al.*, First Experimental Characterization of Microwave Emission from Cosmic Ray Air Showers, Phys. Rev. Lett. **113**, 221101 (2014).

[19] A. Aab *et al.* (Pierre Auger Collaboration), Improved limit to the diffuse flux of ultrahigh energy neutrinos from the Pierre Auger Observatory, Phys. Rev. D **91**, 092008 (2015).
[20] P. Allison *et al.* (ANITA Collaboration), Constraints on the diffuse high-energy neutrino flux from the third flight of ANITA, Phys. Rev. D **98**, 022001 (2018).
[21] A. Romero-Wolf, S. Hoover, A. G. Vieregg *et al.* (ANITA Collaboration), An interferometric analysis method for radio impulses from ultra-high energy particle showers, Astropart. Phys. **60**, 72 (2015).
[22] P. Allison *et al.* (ANITA Collaboration), Dynamic tunable notch filters for the Antarctic impulsive transient antenna (ANITA), Nucl. Instrum. Methods Phys. Res., Sect. A **894**, 47 (2018).
[23] J. A. Högbom, Aperture synthesis with a non-regular distribution of interferometer baselines, Astrophys. J. Suppl. Ser. **15**, 417 (1974).
[24] Han Deng, J. Li, L. Yang, and T. Talty, Intra-vehicle UWB MIMO channel capacity, in *Proceedings of the 2012 IEEE Wireless Communications and Networking Conference Workshops (WCNCW), Paris* (2012), pp. 393–397, https://doi.org/10.1109/WCNCW.2012.6215529.
[25] A. Chandra *et al.*, Serial subtractive deconvolution algorithms for time-domain ultra wide band in-vehicle channel sounding, IET Intell. Transp. Syst. **9**, 870 (2015).
[26] N. Wiener, *Extrapolation, Interpolation, and Smoothing of Stationary Time Series* (Wiley, New York, 1949), ISBN 978-0-262-73005-1.
[27] R. Neelamani, H. Choi, and R. Baraniuk, ForWaRD: Fourier-wavelet regularized deconvolution for ill-conditioned systems, IEEE Trans. Signal Process. **52**, 418 (2004).
[28] D. Bhattacharya, *Harmonic Analysis Techniques in Nonlinear Dispersive Equations and Signal Processing* (ProQuest Dissertations and Theses, 2020), ISBN 9798645447168.
[29] P. Cao, A search for astrophysical ultra high energy neutrinos with the ANITA-IV experiment, Ph.D. thesis dissertation, University of Delaware, ProQuest Dissertations Publishing, 13425957, 2018.
[30] G. A. Hajj, E. R. Kursinski, L. J. Romans, W. I. Bertiger, and S. S. Leroy, A technical description of atmospheric sounding by GPS occultation, J. Atmos. Sol. Terr. Phys. **64**, 451 (2002).
[31] J. M. Aparicio, E. Cardellach, and H. Rodrguez, Information content in reflected signals during GPS Radio Occultation observation, Atmos. Meas. Tech. **11**, 1883 (2018).
[32] S. Y. van der Werf, Noninverted images in inferior mirages, Appl. Opt. **50**, F12 (2011).
[33] A. V. Olinto *et al.*, POEMMA: Probe Of extreme multi-messenger astrophysics, in *Proceedings of 35th International Cosmic Ray Conference, ICRC2017, Busan, Korea* (Sissa Medialab srl, Trieste, 2017).
[34] P. Allison *et al.* (PUEO Collaboration), The payload for ultrahigh energy observations (PUEO): A white paper, arXiv:2010.02892.
[35] M. Tueros (GRAND Collaboration), GRAND, a giant radio array for neutrino detection: Objectives, design and current status, EPJ Web Conf. **216**, 01006 (2019).
[36] A. Romero-Wolf *et al.* (ANITA Collaboration), Comprehensive analysis of anomalous ANITA events disfavors a diffuse tau-neutrino flux origin, Phys. Rev. D **99**, 063011 (2019).